

## UV-induced generation of rare tautomers of allopurinol and 9-methylhypoxanthine — A matrix isolation FTIR study

A. Gerega<sup>a</sup>, L. Lapinski<sup>a</sup>, I. Reva<sup>a,b</sup>, H. Rostkowska<sup>a</sup>, M.J. Nowak<sup>a,\*</sup>

<sup>a</sup> *Institute of Physics, Polish Academy of Sciences, Al. Lotnikow 32/46, 02-668 Warsaw, Poland*

<sup>b</sup> *Department of Chemistry, University of Coimbra, 3004-535 Coimbra, Portugal*

Received 20 December 2005; received in revised form 3 March 2006; accepted 6 March 2006

Available online 10 March 2006

### Abstract

Monomers of allopurinol and 9-methylhypoxanthine were studied using the matrix isolation technique combined with Fourier transform infrared spectroscopy. The oxo tautomeric forms of both compounds were found to dominate in freshly deposited low-temperature argon matrices. For 9-methylhypoxanthine, a small amount of the hydroxy tautomer was also detected in an Ar matrix before any irradiation. Upon exposure of the matrices to the UV ( $\lambda > 230$  nm or  $\lambda > 270$  nm) light, a proton transfer photoreaction converting the oxo forms of both compounds into the corresponding hydroxy tautomers occurred. Generation of conjugated ketenes as minor photoproducts was also observed. For 4(3*H*)-pyrimidinone (a model compound for both allopurinol and 9-methylhypoxanthine), photoreversibility of the UV-induced oxo  $\rightarrow$  hydroxy transformation was experimentally proven by direct observation of the back hydroxy  $\rightarrow$  oxo photoreaction. The substrates (oxo tautomers) and products (hydroxy tautomers) of the observed phototransformations were identified by comparison of their IR spectra with the spectra theoretically predicted at the DFT(B3LYP)/6-31++G(d,p) level. The IR bands in the experimental spectra were assigned to the calculated normal modes.

© 2006 Elsevier B.V. All rights reserved.

**Keywords:** Hypoxanthine; Inosine; Allopurinol; Tautomerism; Photochemistry; Matrix isolation; 9-methylhypoxanthine; 4(3*H*)-pyrimidinone; FTIR spectroscopy; DFT calculations

### 1. Introduction

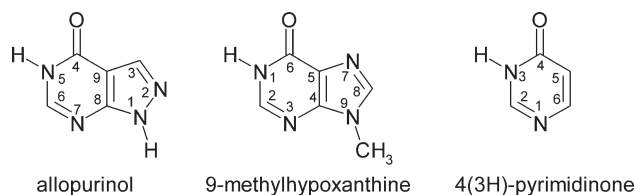
Hypoxanthine is a base of the rare, naturally-occurring nucleoside inosine. This nucleoside appears quite frequently in the anticodon region of natural tRNAs [1]. Since inosine at the 5' end of the anticodon in tRNA does not have a strict base pairing requirements and can form “wobble pairs” with several bases at the 3' end of the codon, it contributes to the degeneracy of the genetic code [2]. Inosine is also commonly present in eukaryotic and prokaryotic messenger-RNA, where it is formed (during post-transcriptional editing) by adenosine-to-inosine enzymatic conversion. Inosine monophosphate plays a key role in both biosynthesis and catabolism of purine nucleosides [3]. Hypoxanthine is present in muscles and

other tissues, where it is formed during purine catabolism by deamination of adenine. This compound also contributes to strong heart muscle contraction and to blood flow in the coronary arteries. As a supplement taken before and during workouts and competition, hypoxanthine stimulates enzyme activity in both cardiac and skeletal muscle cells for improved regeneration of ATP. Inosine ameliorates skeletal muscle ischemia–reperfusion injury, which makes it a potential candidate for therapeutic modulation of skeletal muscle reperfusion injury in the clinical setting [4].

Allopurinol is a heterocyclic molecule, closely related to hypoxanthine. This compound is an inhibitor of xanthine oxidase, which catalyses the conversion of hypoxanthine to xanthine, thus reducing high levels of uric acid in blood and serum. Such a property found application in medications used to prevent gout attacks and to treat hyperuricemia [5–10]. Allopurinol is also used as chemoprotector during anticancer cytotoxic therapies [11,12]. Moreover, this compound is known to effectively protect the heart against damage caused by

\* Corresponding author. Tel.: +48 22 8436601x3219; fax: +48 22 8430926.

E-mail address: [mjnowak@ifpan.edu.pl](mailto:mjnowak@ifpan.edu.pl) (M.J. Nowak).

Scheme 1. Structures and atom numbering of the most stable forms of allopurinol, 9-methylhypoxanthine and 4(3*H*)-pyrimidinone.

oxygen free radicals in patients undergoing cardiac bypass surgery and coronary angioplasty [13–17]. Preliminary results of treatment of bipolar mania and schizophrenia suggest that allopurinol may be an effective adjuvant agent in the treatment of patients with these diseases [18,19].

The structure of crystalline allopurinol was previously determined [20] by the analysis of the X-ray diffraction data. Electronic absorption, dispersed fluorescence, and fluorescence excitation spectra were measured for this compound in aqueous solutions of different pH [21]. These studies revealed that in water solutions the molecules of allopurinol adopt oxo tautomeric forms. The Raman and IR spectra recorded for crystalline allopurinol indicated the presence of the oxo tautomers also in the solid state [22]. Coexistence of the oxo-N(1)H and the oxo-N(2)H tautomers of allopurinol in DMSO solution was suggested on the basis of the  $^{13}\text{C}$  NMR spectroscopic measurements [23].

The experimental physicochemical investigations on inosine and the model hypoxanthine derivatives substituted at N(9) atom (such as 9-methylhypoxanthine) concern mostly the organometallic complexes of these species [24,25]. The photoelectron spectra of gaseous hypoxanthines methylated at different positions (including 9-methylhypoxanthine) have been measured [26]. Although this type of measurements gives usually only rough information about tautomerism, the authors concluded that the oxo forms of the investigated species predominate. As for inosine, its structure in the solid state has been determined using the X-ray crystallographic methods [27].

In the present work monomers of allopurinol and 9-methylhypoxanthine (Scheme 1) isolated in low-temperature argon matrices were investigated using FTIR spectroscopy. Changes induced by UV irradiation of the matrices (decrease of populations of oxo tautomers and increase of populations of hydroxy tautomers) were observed for both compounds. For the sake of comparison, photochemical behavior of a model compound (4(3*H*)-pyrimidinone, Scheme 1) was also taken into consideration.

## 2. Experimental section

Allopurinol and 4(3*H*)-pyrimidinone used in the present study were commercial products supplied by Aldrich. A sample of 9-methylhypoxanthine was kindly made available by Professor Bernhard Lippert (Fachbereich Chemie, Universität Dortmund, Germany). To prepare a low-temperature matrix, the solid sample of a studied compound was electrically heated in a glass miniature oven placed in the vacuum chamber of a continuous-flow helium cryostat. The vapors of the compound were deposited, together with a large excess of inert gas (argon), on a CsI window cooled to 10 K. The argon matrix gas of spectral purity 6.0 was supplied by Linde AG. The IR spectra were recorded with  $0.5\text{ cm}^{-1}$  resolution using the Thermo Nicolet Nexus 670 FTIR spectrometer equipped with a KBr beam splitter and a DTGS detector. Intensities of the IR absorption bands were measured by numerical integration. Matrices were irradiated with light from HBO200 high-pressure mercury lamp. This lamp was fitted with a water filter (to remove

Table 1  
Relative electronic ( $\Delta E_{\text{el}}$ ), zero-point vibrational ( $\Delta ZPE$ ) and total ( $\Delta E_{\text{total}} = \Delta E_{\text{el}} + \Delta ZPE$ ) energies ( $\text{kJ mol}^{-1}$ ) of allopurinol isomers

	AI	AII	AIIIa	AIIIb	AIVa	AV	AVI	AIVb
$\Delta E_{\text{el}}$ (DFT)	0	14.8	23.2	47.8	52.3	53.5	76.5	82.0
$\Delta E_{\text{el}}$ (MP2)	0	11.4	20.1					
$\Delta ZPE$ (DFT)	0	0.0	-0.5	-1.6	-0.4	-1.4	-3.5	-2.0
$\Delta E_{\text{total}}$ (DFT)	0	14.8	22.7	46.2	51.9	52.1	73.0	80.0
$\Delta E_{\text{total}}$ (MP2)*	0	11.4	19.6					

The energy of the form AI was taken as reference. The results of calculations obtained using the 6-31++G(d,p) basis set.

\* $\Delta E_{\text{total}}$ (MP2) was obtained using MP2 values of  $\Delta E_{\text{el}}$  and DFT(B3LYP) values of  $\Delta ZPE$ .

Electronic energies obtained for the form AI are:  $E_{\text{el}}$ (DFT) = -487.201604 hartree,  $E_{\text{el}}$ (MP2) = -487.005774 hartree.

Zero-point vibrational energy ZPE obtained at the DFT level for the form AI is  $263.3\text{ kJ mol}^{-1}$ .

IR radiation) and a suitable cutoff filter UG11 or UG5 (Schott) transmitting light with  $\lambda > 270$  nm or with  $\lambda > 230$  nm, respectively.

### 3. Computational section

The geometries of isomers of allopurinol, 9-methylhypoxanthine and 4(3*H*)-pyrimidinone considered in this work were optimized using the hybrid Hartree–Fock and density functional theory method DFT(B3LYP) with the Becke's three-parameter exchange functional [28] and gradient-corrected functional of Lee et al. [29]. At the optimized geometries, the DFT(B3LYP) harmonic vibrational frequencies and IR intensities were calculated at the same theory level. To correct for the systematic shortcomings of the applied methodology (mainly for anharmonicity), the predicted vibrational wavenumbers were scaled down by a single factor of 0.98. The theoretical normal modes, calculated for the tautomers of the studied compounds were analyzed by carrying out the potential energy distribution (PED) calculation. Transformations of the force constants with respect to the Cartesian coordinates to the force constants with respect to the molecule-fixed internal coordinates allowed the normal-coordinate analysis to be performed as described by Schachtschneider [30]. The internal coordinates used in this analysis were defined following the recommendations of Pulay et al. [31]. These coordinates are listed in Tables S1 and S2 (in the Supplementary data). Potential energy distribution (PED) matrices [32] have been calculated and the elements of these matrices greater than 10% are given in Tables 2, 3, 5 and 6.

It is commonly known that the DFT method reproduces well the infrared spectra but provides less reliable values of relative electronic energies. That is why the relative energies of the most stable isomeric forms of allopurinol were also calculated using the MP2 method at equilibrium geometries fully optimized at this level of theory [33]. The same procedures were applied to calculate the relative energies of the most stable isomeric forms of 9-methylhypoxanthine.

All quantum-mechanical calculations were performed with the GAUSSIAN 98 program [34] using the 6-31++G(d,p) basis set.

### 4. Results

#### 4.1. Allopurinol

The tautomerism of allopurinol is determined by the positions of two labile hydrogen atoms in the molecule. For this compound, there are 9 tautomers with canonical structures. These forms are presented in Scheme S1 in the Supplementary data. The relative energies of the tautomeric forms of allopurinol were calculated at the DFT(B3LYP) and MP2 levels. These calculations predict that the oxo tautomer AI with one of the labile hydrogens attached to N(1) and the other to N(5) nitrogen atoms is the most stable. The relative energies of five other tautomers (AII, AIII, AIV, AV, AVI) are given in Table 1. The forms not listed in this table are very high in energy (by more than  $100 \text{ kJ mol}^{-1}$ ) and can be safely ruled out from further discussion.

Among the low-energy isomers of allopurinol (listed in Table 1), the oxo tautomer AII is higher in energy by  $11.4 \text{ kJ mol}^{-1}$  (MP2), with respect to the energy of the oxo tautomer AI. The energy difference between the most stable hydroxy form AIIIa and tautomer AI is considerably high and is equal  $20.1 \text{ kJ mol}^{-1}$  (MP2). Previous theoretical calculations of relative energies of allopurinol tautomers, carried out at a lower level, led to similar predictions [35,36]. Hence, for the gaseous allopurinol at ca. 450 K, the tautomeric form AI is expected to dominate, whereas tautomer AII can be populated only in a very small amount. The thermal population of any of the hydroxy tautomers should be so low that these forms would not be detectable either in the gas phase or in the low-temperature matrices.

The infrared spectrum of allopurinol monomers isolated in an argon matrix is presented in Fig. 1. In the high-frequency region, two bands due to the NH stretching vibrations of the oxo form were observed at  $3491$  and  $3432/3430 \text{ cm}^{-1}$ . These bands

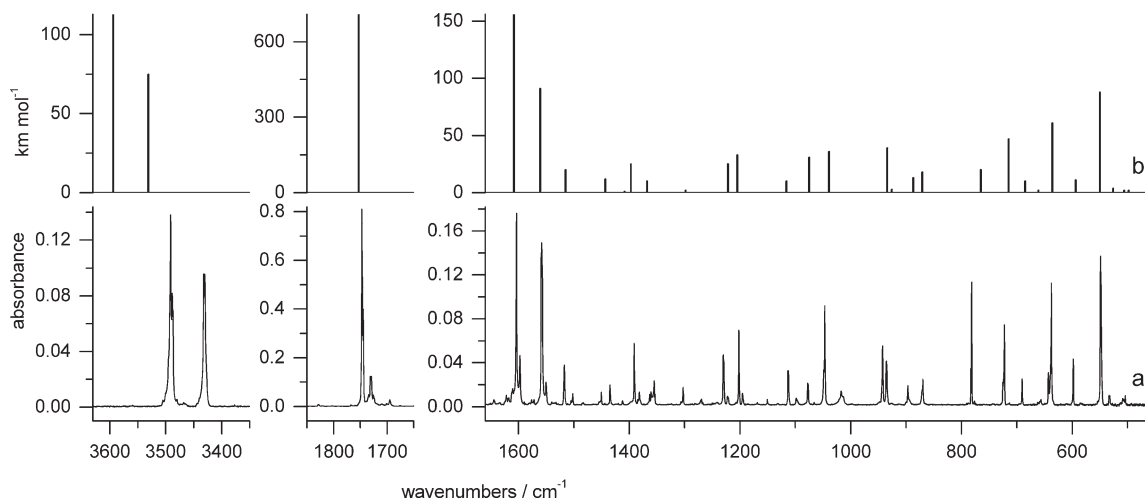


Fig. 1. Comparison of (a) the experimental IR absorption spectrum of allopurinol isolated in an Ar matrix with (b) the spectrum of the oxo tautomer AI theoretically simulated at the DFT(B3LYP)/6-31++G(d,p) level. The calculated wavenumbers were scaled by a factor of 0.98.

should correspond to the  $\nu\text{N1H}$  vibration in the pyrazole ring and to the  $\nu\text{N5H}$  vibration in the pyrimidine ring, respectively. The frequency of the latter band due to the stretching N5H vibration is very close to that of the corresponding  $\nu\text{N3H}$  band ( $3428\text{ cm}^{-1}$ ), which was observed in the IR spectrum of 4(3*H*)-pyrimidinone isolated in an Ar matrix [37]. It indicates that this

band is due to the stretching vibration of the NH group in the pyrimidine ring.

No absorption was found in frequency range  $3650\text{--}3550\text{ cm}^{-1}$ , where the bands due to the OH stretching vibrations should be expected. The absence of the  $\nu\text{OH}$  band in the IR spectrum of allopurinol indicates that only oxo tautomer(s) of the

Table 2  
Experimental wavenumbers ( $\tilde{\nu}/\text{cm}^{-1}$ ) and relative integral intensities ( $I$ ) of the absorption bands in the spectrum of allopurinol isolated in an Ar matrix, compared with wavenumbers ( $\tilde{\nu}/\text{cm}^{-1}$ ), absolute intensities ( $A^{\text{th}}/\text{km mol}^{-1}$ ) and potential energy distribution (PED, %) calculated for the oxo form AI

Experimental Ar matrix		Calculated B3LYP/6-31++G(d,p)		
$\tilde{\nu}$	$I^{\text{a}}$	$\tilde{\nu}^{\text{b}}$	$A^{\text{th}}$	PED <sup>c</sup> (%)
<b>3491</b> 3488	163	3594	113	$\nu\text{N1H}$ (100)
3432 3430	113	3531	75	$\nu\text{N5H}$ (100)
		3209	0	$\nu\text{C3H}$ (99)
		3135	4	$\nu\text{C6H}$ (100)
<b>1747</b> 1744 1730 1725	607	1753	710	$\nu\text{CO}$ (72), $\nu\text{C4C9}$ (13)
1695	33			
1644	3			
1610 <b>1603</b> 1597	110	1608	156	$\nu\text{C6N7}$ (53), $\beta\text{C6H}$ (13)
<b>1558</b> 1550	115	1561	91	$\nu\text{N7C8}$ (26), $\nu\text{C8C9}$ (22), $\beta\text{N1H}$ (18), $\nu\text{N1C8}$ (13)
1517	16	1515	20	$\nu\text{N1C8}$ (18), $\nu\text{C3C9}$ (16), $\beta\text{C3H}$ (11)
1502	4			
1450	4			
1434	7	1443	12	$\nu\text{N2C3}$ (21), $\beta\text{N5H}$ (16), $\beta\text{N1H}$ (11), $\nu\text{N5C6}$ (10)
1412	1	1408	1	$\beta\text{N5H}$ (24), $\nu\text{C8C9}$ (20), $\nu\text{N1C8}$ (16), $\nu\text{N5C6}$ (10)
1391	21	1397	25	$\nu\text{N2C3}$ (28), $\nu\text{C3C9}$ (20), $\nu\text{C4C9}$ (13), $\beta\text{N5H}$ (10)
1382	7			
1363 1360 <b>1355</b>	21	1368	10	$\beta\text{C6H}$ (57), $\nu\text{C6N7}$ (11), $\nu\text{N2C3}$ (10)
1303	7	1298	2	$\beta\text{N1H}$ (45), $\nu\text{N1C8}$ (10)
1269	3			
<b>1230</b> 1222	28	1222	25	$\beta\text{C3H}$ (26), $\beta\text{R5}$ (24), $\nu\text{C4C9}$ (16)
<b>1202</b> 1196	27	1205	33	$\beta\text{C3H}$ (33), $\nu\text{C3C9}$ (12)
1169	1			
1151	2			
1118 1112	15	1116	10	$\nu\text{N5C6}$ (43), $\beta\text{N5H}$ (22)
1098	4			
1077	10	1075	31	$\nu\text{N1N2}$ (59)
1066	1			
1047	43	1039	36	$\nu\text{C4N5}$ (32), $\beta\text{CO}$ (16), $\nu\text{N1N2}$ (12)
<b>1017</b> 1013	16			
942	25	934	39	$\beta\text{R4}$ (61), $\nu\text{C8C9}$ (13)
935	22	926	3	$\gamma\text{C6H}$ (107)
897	10	887	13	$\beta\text{R1}$ (51), $\beta\text{R2}$ (12)
870	13	871	18	$\gamma\text{C3H}$ (103)
783 <b>781</b>	31	765	20	$\gamma\text{CO}$ (37), $\tau\text{R1}$ (37), $\tau\text{R4}$ (19)
725 <b>723</b>	28	715	47	$\gamma\text{CO}$ (42), $\gamma\text{N5H}$ (34), $\tau\text{R5}$ (14)
691	8	685	10	$\nu\text{N7C8}$ (22), $\nu\text{C4N5}$ (19), $\nu\text{N1C8}$ (10)
662	3	661	2	$\tau\text{R5}$ (54), $\tau\text{R4}$ (25), $\gamma\text{N5H}$ (19)
656	3			
643 <b>637</b>	57	636	61	$\gamma\text{N5H}$ (42), $\tau\text{R4}$ (30), $\tau\text{R3}$ (15), $\gamma\text{CO}$ (11)
598	12	594	11	$\beta\text{R5}$ (28), $\nu\text{C4C9}$ (19), $\beta\text{R2}$ (12), $\beta\text{CO}$ (11)
549	70	550	88	$\gamma\text{N1H}$ (54), $\tau\text{R2}$ (17), $\tau\text{R4}$ (16), $\tau\text{R1}$ (15)
<b>534</b> 532	4	526	4	$\beta\text{R2}$ (37), $\beta\text{CO}$ (23), $\nu\text{C4N5}$ (10), $\beta\text{R1}$ (10)
<b>509</b> 507	3	506	2	$\gamma\text{N1H}$ (42), $\tau\text{R2}$ (25), $\tau\text{R5}$ (15), $\tau\text{R1}$ (13)
504	3	498	2	$\beta\text{R3}$ (68)
		307	3	$\beta\text{CO}$ (34), $\beta\text{R2}$ (18), $\nu\text{C4C9}$ (13)
		261	0	$\tau\text{R3}$ (57), $\tau\text{RR}$ (19), $\tau\text{R5}$ (14), $\tau\text{R4}$ (10)
		192	2	$\tau\text{RR}$ (63), $\tau\text{R3}$ (25)
		154	6	$\tau\text{R2}$ (59), $\tau\text{R1}$ (28), $\tau\text{R3}$ (10)

Wavenumbers of the strongest components of split bands are bold.

<sup>a</sup> Relative integrated intensities.

<sup>b</sup> Theoretical positions of absorption bands were scaled down by a factor of 0.98.

<sup>c</sup> PED's lower than 10% are not included. Definition of internal coordinates is given in Table S1. See Scheme 1 for atom numbering.

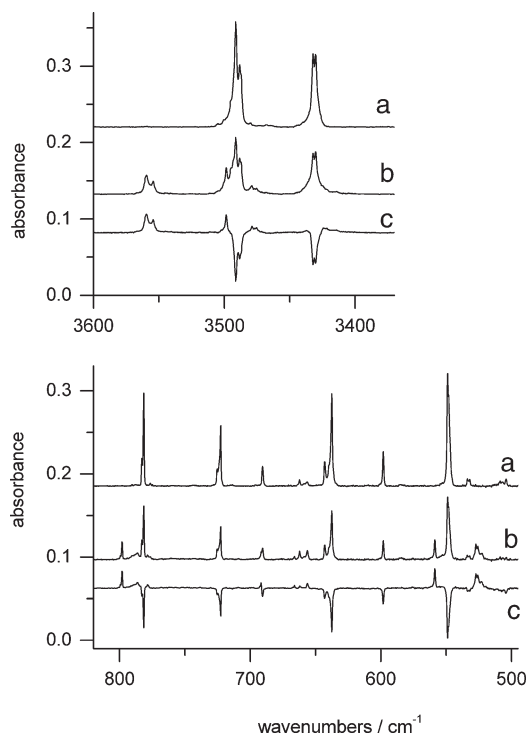
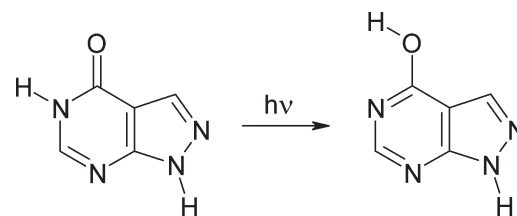


Fig. 2. Portions of the IR spectrum of allopurinol isolated in an Ar matrix recorded: (a) after deposition; (b) after 4 h of UV ( $\lambda > 230$  nm) irradiation; (c) difference spectrum: trace b minus trace a.

compound exist(s) in the Ar matrix after its deposition. The comparison of the experimental IR spectrum of allopurinol isolated in a low-temperature Ar matrix with the spectrum theoretically predicted (at the DFT(B3LYP)/6-31++G(d,p) level) for isomer AI is presented in Fig. 1. Good agreement between the patterns of experimental and theoretical spectra supports the conclusion that the oxo tautomeric form AI is adopted by allopurinol monomers isolated in an Ar matrix. Assignment of the observed absorption bands to the theoretically predicted normal modes of tautomer AI of the compound is given in Table 2.



Scheme 2. Phototautomeric reaction observed for allopurinol.

Comparison of the experimental spectrum of allopurinol with the spectra calculated for tautomers AI and AII does not allow to unequivocally assign any band, in the whole mid-IR range, to tautomer AII. Hence, there are no clear spectral signatures of the presence of this form in a low-temperature Ar matrix. On the other hand, the presence of a very small amount of allopurinol adopting the tautomeric form AII cannot be excluded based on the present experimental observations.

Upon UV ( $\lambda > 230$  nm) irradiation of the monomers of the compound isolated in an Ar matrix, all the bands of the initial spectrum (including the most intense  $\nu\text{C}=\text{O}$  band at  $1747\text{ cm}^{-1}$ ) decreased, whereas a new spectrum of photoproduct(s) emerged (see Fig. 2). The appealing feature of this new spectrum is the presence of the band at  $3559\text{ cm}^{-1}$ , which can be assigned to the stretching vibration of the OH group ( $\nu\text{OH}$ ). The position of this band is quite similar to that of the  $\nu\text{OH}$  band found previously at  $3564\text{ cm}^{-1}$  in the spectrum of 4-hydroxypyrimidine [37–39]. On the basis of this observation one can postulate that the oxo (AI)  $\rightarrow$  hydroxy (AIIIa) photoreaction (Scheme 2) occurred for the monomers of allopurinol isolated in a low-temperature matrix. Photoreaction of the same type was previously observed for matrix-isolated 4(3H)-pyrimidinone [38–40], see also the forthcoming section of the current paper.

The photoprocess induced by UV ( $\lambda > 230$  nm) irradiation of monomeric allopurinol did not lead to total conversion of the oxo form AI into the hydroxy tautomer AIIIa (for the structure see Table 1). Upon prolonged (4 h) UV irradiation the intensities of the IR bands due to AI substrate decreased to 48% of their initial

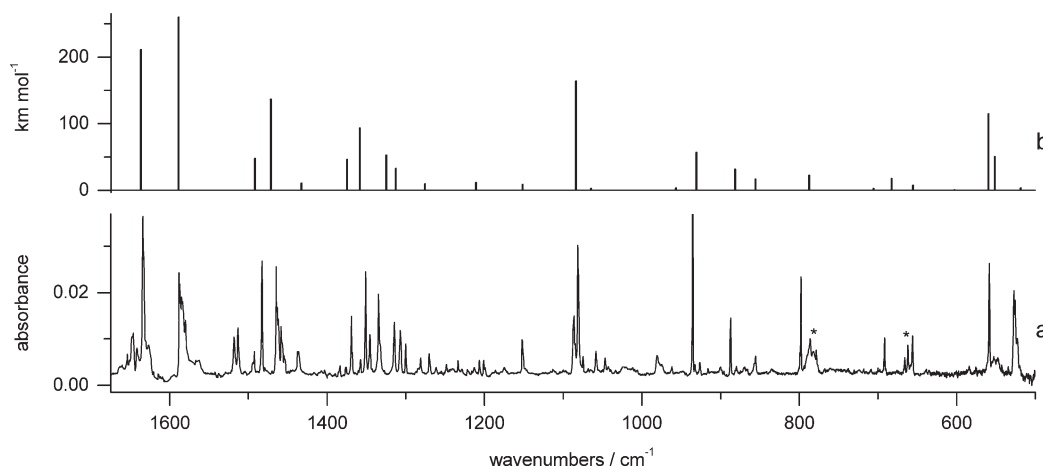


Fig. 3. Comparison of (a) the experimental spectrum of the photoproducts generated upon UV ( $\lambda > 230$  nm) irradiation of allopurinol isolated in an Ar matrix with (b) the spectrum of the hydroxy tautomeric form AIIIa theoretically simulated at the DFT(B3LYP)/6-31++G(d,p) level. The calculated wavenumbers were scaled by a factor of 0.98. Asterisks in the experimental spectrum point to the bands which indicate UV-induced creation of the ketene form with the open pyrimidine ring. The spectrum of unreacted oxo tautomer AI was subtracted.

values. Hence, 52% of the AI form was converted into photoproduct(s) (Fig. 2). The extracted spectrum of the photoproduct(s) is compared in Fig. 3 with the spectrum of the hydroxy form AIIIa theoretically predicted at the DFT(B3LYP)/6-31++G(d,p) level. Good overall agreement between these two spectra supports the conclusion that the main photogenerated species is tautomer AIII. No such agreement was observed between the experimental spectrum of the photoproduct(s) and

the theoretical spectra of other hydroxy isomers; e.g. form AIVa (see Fig. S1 in the Supplementary data). The assignment of the observed absorption bands to the theoretically calculated normal modes of the form AIIIa is given in Table 3.

A minor product emerging after UV irradiation of the matrix and coexisting with the dominating photoproduct AIII has a characteristic, comparatively broad band at  $2153\text{ cm}^{-1}$  (Fig. 4). The frequency, complex pattern with many maxima, and high

Table 3  
Experimental wavenumbers ( $\tilde{\nu}/\text{cm}^{-1}$ ) and relative integral intensities ( $I$ ) of the absorption bands in the spectrum of the form photoproducted upon UV irradiation of allolpurinol isolated in an Ar matrix, compared with wavenumbers ( $\tilde{\nu}/\text{cm}^{-1}$ ), absolute intensities ( $A^{\text{th}}/\text{km mol}^{-1}$ ) and potential energy distribution (PED, %) calculated for the hydroxy form AIIIa

Experimental Ar matrix		Calculated B3LYP/6-31++G(d,p)		
$\tilde{\nu}$	$I^a$	$\tilde{\nu}^b$	$A^{\text{th}}$	PED <sup>c</sup> (%)
<b>3559</b> 3555	189	3676	108	$\nu\text{OH}$ (100)
<b>3498</b> 3495	180	3601	117	$\nu\text{N1H}$ (100)
3479	60			
		3206	1	$\nu\text{C3H}$ (99)
		3137	13	$\nu\text{C6H}$ (100)
1646 1642 <b>1634</b>	193	1637	211	$\nu\text{C4C9}$ (34), $\nu\text{N7C8}$ (11), $\nu\text{C3C9}$ (10)
<b>1588</b> 1585 1580	160	1589	260	$\nu\text{C8C9}$ (21), $\nu\text{N7C8}$ (17), $\beta\text{N1H}$ (10)
1518 1513	45			
1493	11			
1483	43	1492	48	$\nu\text{C4N5}$ (17), $\beta\text{C6H}$ (17), $\nu\text{N2C3}$ (14), $\nu\text{N1C8}$ (13)
<b>1465</b> 1462 1459 1455	108	1472	137	$\nu\text{N2C3}$ (30), $\nu\text{CO}$ (16), $\nu\text{C4N5}$ (11)
1437	15	1433	11	$\nu\text{N1C8}$ (27), $\beta\text{N1H}$ (17), $\beta\text{C6H}$ (14), $\nu\text{C8C9}$ (12)
1369	19	1375	47	$\beta\text{C6H}$ (24), $\nu\text{C8C9}$ (16), $\nu\text{N2C3}$ (14), $\nu\text{CO}$ (11)
1358	6			
<b>1351</b> 1346	57	1359	94	$\nu\text{C6N7}$ (29), $\nu\text{C3C9}$ (21), $\nu\text{N7C9}$ (12)
1335	49	1325	53	$\nu\text{C6N7}$ (20), $\beta\text{OH}$ (17), $\nu\text{C4N5}$ (12), $\nu\text{C3C9}$ (12), $\nu\text{N2C3}$ (11)
1315 1307	43	1313	33	$\nu\text{N5C6}$ (22), $\beta\text{C6H}$ (21), $\beta\text{OH}$ (14), $\beta\text{N1H}$ (11), $\nu\text{CO}$ (10)
1300	9			
1271	9	1276	10	$\beta\text{N1H}$ (29), $\nu\text{N5C6}$ (12), $\beta\text{OH}$ (11)
1262	3			
1249	5			
1234	3			
1207	4			
<b>1201</b> 1199	8	1211	12	$\beta\text{C3H}$ (49), $\beta\text{OH}$ (15)
1152	19	1152	9	$\beta\text{R5}$ (22), $\nu\text{N5C6}$ (17)
1087 <b>1081</b>	104	1084	164	$\beta\text{OH}$ (17), $\nu\text{C4N5}$ (16), $\nu\text{N1N2}$ (14), $\nu\text{N5C6}$ (13)
1059	10	1065	3	$\nu\text{N1N2}$ (61)
<b>981</b> 976	26	957	4	$\gamma\text{C6H}$ (108)
936	53	931	57	$\beta\text{R4}$ (60), $\nu\text{C8C9}$ (16)
926	5			
887	21	882	32	$\beta\text{R1}$ (49), $\beta\text{R2}$ (19)
<b>857</b> <b>856</b>	10	856	17	$\gamma\text{C3H}$ (101)
798	27	788	23	$\tau\text{R1}$ (56), $\gamma\text{CO}$ (19), $\tau\text{R4}$ (16)
		706	3	$\nu\text{N7C8}$ (21), $\beta\text{R5}$ (10)
692	10	683	18	$\gamma\text{CO}$ (47), $\tau\text{R5}$ (24), $\tau\text{RR}$ (14), $\tau\text{R3}$ (10)
656	19	656	8	$\tau\text{R4}$ (55), $\tau\text{R5}$ (37)
		603	1	$\beta\text{R5}$ (30), $\nu\text{C4C9}$ (20), $\beta\text{R2}$ (14)
559	38	560	115	$\tau\text{OH}$ (22), $\tau\text{R2}$ (21), $\tau\text{R1}$ (17), $\gamma\text{N1H}$ (15)
<b>527</b> 526 523	79	552	51	$\tau\text{OH}$ (70), $\tau\text{R1}$ (10)
		521	0	$\beta\text{R3}$ (51), $\beta\text{R2}$ (23)
		519	4	$\beta\text{CO}$ (32), $\beta\text{R2}$ (16), $\nu\text{N1C8}$ (13), $\beta\text{R3}$ (13)
<b>489</b> 485	21	494	31	$\gamma\text{N1H}$ (81)
		293	5	$\beta\text{CO}$ (44), $\beta\text{R2}$ (12), $\nu\text{C4C9}$ (10)
		292	1	$\tau\text{R3}$ (56), $\tau\text{R5}$ (15), $\tau\text{R4}$ (10)
		203	1	$\tau\text{RR}$ (71), $\tau\text{R3}$ (20)
		166	0	$\tau\text{R2}$ (67), $\tau\text{R1}$ (16), $\gamma\text{CO}$ (11)

Wavenumbers of the strongest components of split bands are bold.

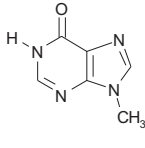
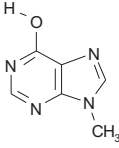
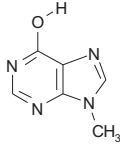
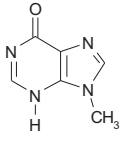
<sup>a</sup> Relative integrated intensities.

<sup>b</sup> Theoretical positions of absorption bands were scaled down by a factor of 0.98.

<sup>c</sup> PED's lower than 10% are not included. Definition of internal coordinates is given in Table S1. See Scheme 1 for atom numbering.

Table 4

Relative electronic ( $\Delta E_{\text{el}}$ ), zero-point vibrational ( $\Delta ZPE$ ) and total ( $\Delta E_{\text{total}} = \Delta E_{\text{el}} + \Delta ZPE$ ) energies ( $\text{kJ mol}^{-1}$ ) of 9-methylhypoxanthine isomers

				
	mHxI	mHxIIa	mHxIIb	mHxIII
$\Delta E_{\text{el}}(\text{DFT})$	0	13.6	18.8	85.9
$\Delta E_{\text{el}}(\text{MP2})$	0	10.3	15.1	
$\Delta ZPE(\text{DFT})$	0	0.0	0.1	-3.7
$\Delta E_{\text{total}}(\text{DFT})$	0	13.6	18.9	82.2
$\Delta E_{\text{total}}(\text{MP2})^*$	0	10.3	15.2	

The energy of the form mHxI was taken as reference. The results of calculations obtained using the 6-31++G(d,p) basis set.

\* $\Delta E_{\text{total}}(\text{MP2})$  was obtained using MP2 values of  $\Delta E_{\text{el}}$  and DFT(B3LYP) values of  $\Delta ZPE$ .

Electronic energies obtained for the form mHxI are:  $E_{\text{el}}(\text{DFT}) = -526.531856$  hartree,  $E_{\text{el}}(\text{MP2}) = -525.040618$  hartree.

Zero-point vibrational energy ZPE obtained at the DFT level for the form mHxI is  $335.5 \text{ kJ mol}^{-1}$ .

intensity are typical of a band due to the “antisymmetric” stretching vibration of the  $-\text{C}=\text{C}=\text{O}$  group [39–41]. The conjugated ketene can exist in several possible stable isomeric forms, one of them is presented in Scheme 3A. For this structure, an extremely intense ( $1116 \text{ km mol}^{-1}$ ) band due to  $-\text{C}=\text{C}=\text{O}$  “antisymmetric” stretching vibration with frequency  $2159 \text{ cm}^{-1}$  was theoretically predicted at the DFT(B3LYP) level. Analogous calculations carried out for other possible stable isomeric forms of open-ring conjugated ketene resulted in predictions of equally strong IR bands at nearly the same ( $\pm 20 \text{ cm}^{-1}$ )

frequency. The comparison between the experimental observation with the theoretically predicted frequency and intensity of the band due to  $-\text{C}=\text{C}=\text{O}$  “antisymmetric” stretching vibration suggests that a ring-opening reaction occurs for allopurinol upon UV irradiation.

#### 4.2. 9-Methylhypoxanthine

Allopurinol and hypoxanthine are isomers. In both compounds one of the rings has the structure of 4(3H)-pyrimidinone and the other has a five-membered structure (pyrazole or imidazole) with two nitrogen atoms. Tautomerism of hypoxanthine has

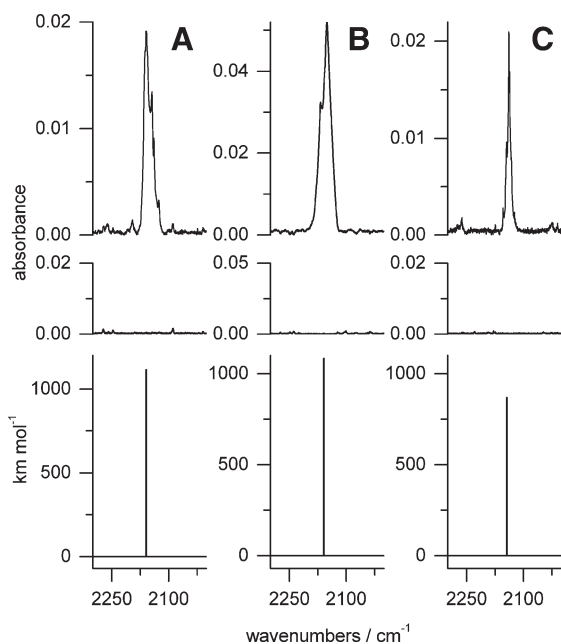


Fig. 4. The spectral range where the bands due to the “antisymmetric” vibrations of the ketene  $-\text{C}=\text{C}=\text{O}$  group should be expected. IR spectra recorded after deposition of matrices are given in the middle row. The spectra recorded after UV irradiation of the matrices are given in the upper row. The spectra theoretically simulated, at the DFT(B3LYP)/6-31++G(d,p) level, for the ketene structures (shown in Scheme 3), are given in the bottom row. The calculated wavenumbers were scaled by a factor of 0.98. The spectra presented in column A concern allopurinol; in column B 9-methylhypoxanthine; in column C 4(3H)-pyrimidinone.

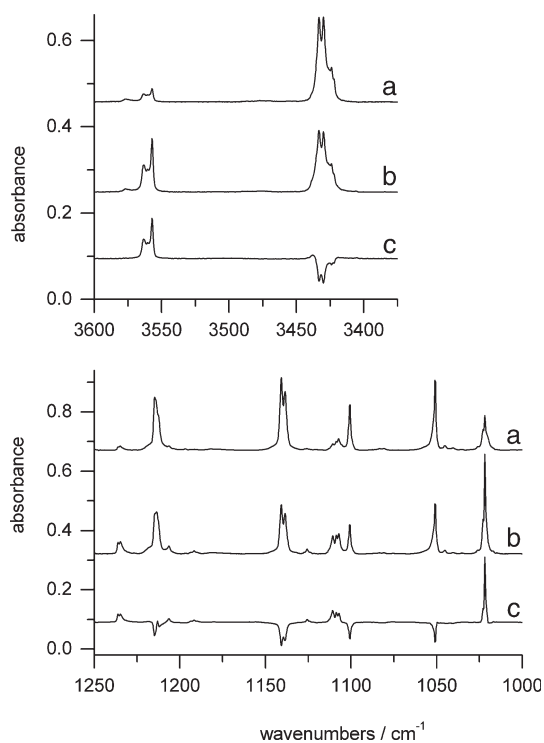


Fig. 5. Portions of the IR spectrum of 9-methylhypoxanthine isolated in an Ar matrix: (a) after deposition of the matrix; (b) after 12 h of UV ( $\lambda > 270 \text{ nm}$ ) irradiation; (c) difference spectrum: trace b minus trace a.

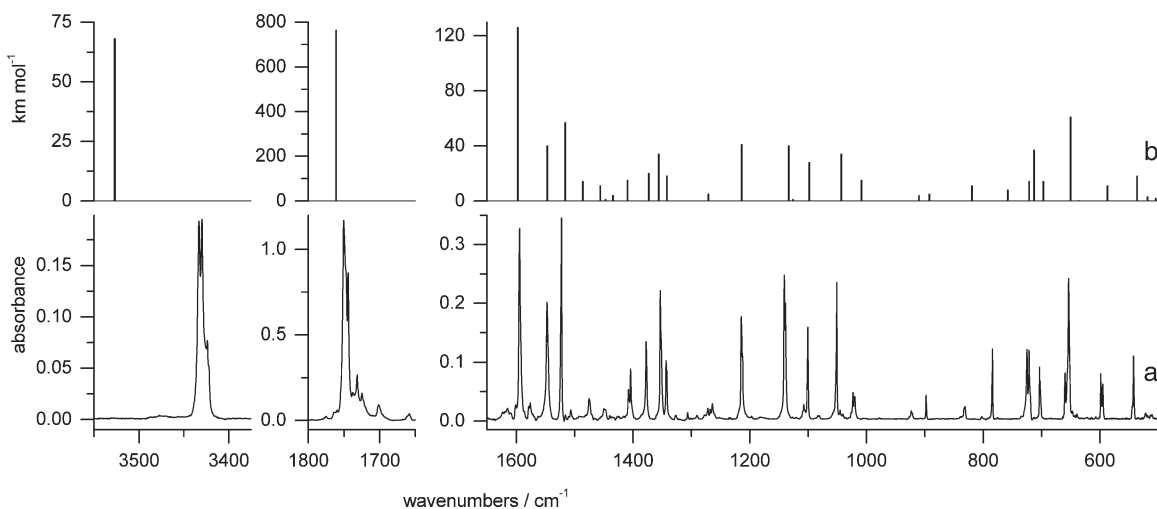


Fig. 6. Comparison of (a) the extracted experimental spectrum of the bands due to the oxo tautomer of 9-methylhypoxanthine dominating in the Ar matrix before UV irradiation with (b) the theoretical spectrum of the oxo tautomer mHxI of 9-methylhypoxanthine calculated at the DFT(B3LYP)/6-31++G(d,p) level. Theoretical wavenumbers were scaled by a factor of 0.98.

been theoretically studied in previous works [35,42–45]. All of these calculations predict the oxo-N(1)H,N(7)H tautomer of hypoxanthine as the most stable form of the compound and the oxo-N(1)H,N(9)H tautomer as the form only slightly (by 3–5 kJ mol<sup>-1</sup>) higher in energy. Both tautomers were detected in the recent experimental investigation of matrix-isolated hypoxanthine [42,43].

Methylation at the N(9) nitrogen atom fixes the form of hypoxanthine in which the compound is present in inosine, its biologically important nucleoside. In 9-methylhypoxanthine the number of possible tautomeric forms is significantly reduced (see Table 4). For this species, there is only one labile hydrogen atom,

which can be attached to either the oxygen atom or to one of the nitrogen atoms of the pyrimidine ring. Theoretical calculations, carried out in the present work at DFT and MP2 levels, show that there are two low-energy forms of 9-methylhypoxanthine (the oxo-N(1)H-tautomer mHxI and the hydroxy tautomer mHxII), whereas the third tautomeric form mHxIII is much higher in energy (see Table 4). The oxo-N(1)H tautomer mHxI was predicted at both applied levels of theory to be the most stable form. The energy of the hydroxy forms mHxIIa and mHxIIb was calculated to be 10–19 kJ mol<sup>-1</sup> higher.

In the high frequency range (3600–3400 cm<sup>-1</sup>) of the experimental spectrum of 9-methylhypoxanthine isolated in an

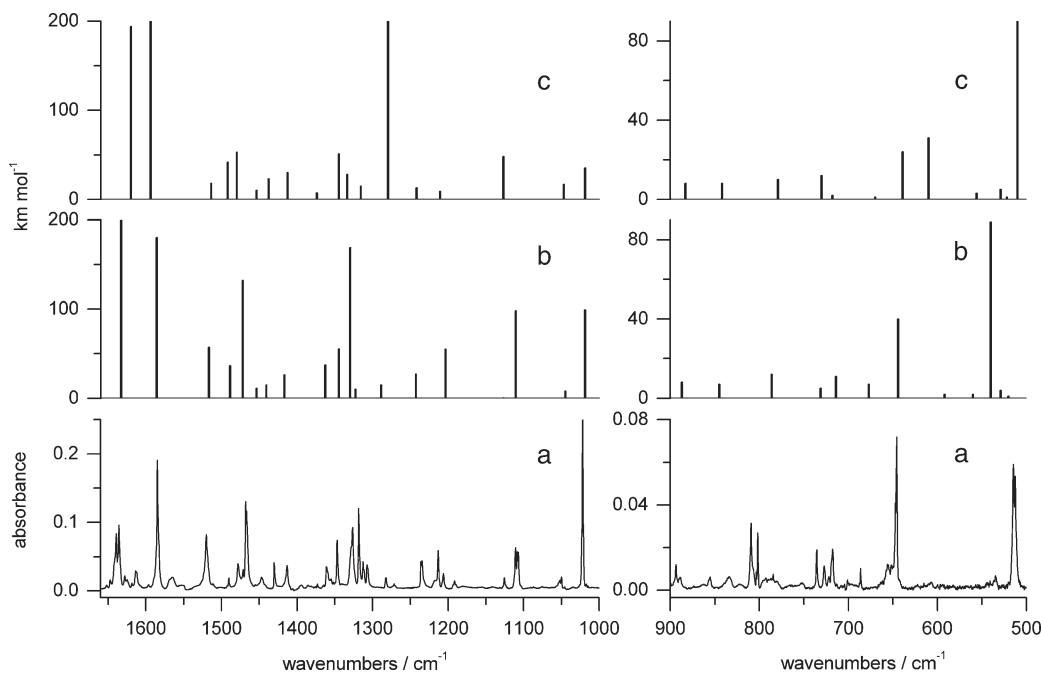


Fig. 7. Comparison of (a) the extracted spectrum of the bands due to the main photoproduct (the hydroxy tautomer) generated upon UV ( $\lambda > 270$  nm) irradiation of 9-methylhypoxanthine isolated in an Ar matrix with (b) the theoretical spectrum of the hydroxy isomer mHxIIa and (c) the theoretical spectrum of the hydroxy isomer mHxIIb. The theoretical spectra were calculated at the DFT(B3LYP)/6-31++G(d,p) level. The calculated wavenumbers were scaled by a factor of 0.98.

Table 5

Experimental wavenumbers ( $\tilde{\nu}/\text{cm}^{-1}$ ) and relative integral intensities ( $I$ ) of the absorption bands in the spectrum of the oxo form of 9-methylhypoxanthine isolated in an Ar matrix, compared with wavenumbers ( $\tilde{\nu}/\text{cm}^{-1}$ ), absolute intensities ( $A^{\text{th}}/\text{km mol}^{-1}$ ) and potential energy distribution (PED, %) calculated for the oxo form mHxI

Experimental Ar matrix		Calculated B3LYP/6-31++G(d,p)		
$\tilde{\nu}$	$I^{\text{a}}$	$\tilde{\nu}^{\text{b}}$	$A^{\text{th}}$	PED <sup>c</sup> (%)
<b>3433 3430</b> 3424 3422	100	3527	68	$\nu\text{N1H}$ (100)
		3190	0	$\nu\text{C8H}$ (99)
3115	1	3136	4	$\nu\text{C2H}$ (100)
2998	3	3095	6	$\nu\text{Me2}$ (93)
2961	9	3073	9	$\nu\text{Me3}$ (93)
2930 2922 2888	11	3002	37	$\nu\text{Me1}$ (98)
1775	8			
1764 1760 <b>1750</b> 1744	583	1761	764	$\nu\text{CO}$ (72), $\nu\text{C5C6}$ (13)
1738 <b>1732</b> 1725	178			
1702	35			
1658	12			
1594	79	1597	126	$\nu\text{C2N3}$ (54), $\beta\text{C2H}$ (15)
1579 1576	8			
1547	51	1547	40	$\nu\text{N3C4}$ (23), $\nu\text{N9C4}$ (18), $\nu\text{N7C8}$ (15), $\nu\text{C4C5}$ (14)
1522	46	1516	57	$\nu\text{C4C5}$ (26)
1506	2			
1475	9	1486	14	$\beta\text{Me2}$ (76), $\beta\text{Me3}$ (11)
<b>1450</b> 1447	6	1456	11	$\beta\text{Me4}$ (89)
		1447	1	$\beta\text{N1H}$ (26), $\nu\text{N7C8}$ (20)
1440	1	1434	4	$\beta\text{Me1}$ (72), $\nu\text{N7C8}$ (11)
1408 <b>1404</b>	19	1409	15	$\nu\text{N7C8}$ (16), $\beta\text{Me1}$ (15), $\beta\text{N1H}$ (13), $\nu\text{N9C4}$ (12), $\nu\text{N1C2}$ (10), $\nu\text{C4C5}$ (10)
1377	25	1373	20	$\beta\text{C2H}$ (26), $\nu\text{C5C6}$ (14), $\nu\text{N9C14}$ (10)
1353	40	1356	34	$\beta\text{C2H}$ (33), $\nu\text{C2N3}$ (18), $\nu\text{C5N7}$ (16)
1343	19	1342	18	$\nu\text{C8N9}$ (25), $\nu\text{C5N7}$ (16)
1290	1			
1272 1268 <b>1264</b>	10	1271	5	$\beta\text{C8H}$ (28), $\nu\text{C8N9}$ (12), $\beta\text{Me3}$ (11)
1215	43	1214	41	$\beta\text{C8H}$ (36), $\nu\text{N9C14}$ (15)
<b>1141</b> 1139	61	1133	40	$\nu\text{N1C2}$ (33), $\beta\text{N1H}$ (19), $\nu\text{C6N1}$ (12)
1127	0	1126	1	$\beta\text{Me5}$ (87)
1101	17	1098	28	$\nu\text{N1C2}$ (17), $\beta\text{R1}$ (16)
1084 <b>1081</b>	1			
<b>1051</b> 1045 1040	34	1043	34	$\beta\text{Me3}$ (45), $\nu\text{C8N9}$ (26), $\beta\text{R4}$ (13)
		1008	15	$\nu\text{C6N1}$ (25), $\beta\text{R4}$ (17), $\beta\text{CO}$ (12), $\beta\text{R5}$ (11)
<b>924</b> 921	3	910	4	$\gamma\text{C2H}$ (107)
899	4	892	5	$\beta\text{R1}$ (47), $\beta\text{R2}$ (10), $\nu\text{C5N7}$ (10)
839 <b>832</b>	6	819	11	$\gamma\text{C8H}$ (100)
784	12	758	8	$\gamma\text{CO}$ (33), $\tau\text{R1}$ (32), $\tau\text{R4}$ (26)
725	8	721	14	$\nu\text{N9C14}$ (31), $\beta\text{R4}$ (28), $\beta\text{R2}$ (13), $\nu\text{C8N9}$ (10)
721	11	713	37	$\gamma\text{N1H}$ (47), $\gamma\text{CO}$ (40)
713	1			
<b>704</b> 702	13	697	14	$\nu\text{N3C4}$ (24), $\nu\text{C6N1}$ (14), $\nu\text{N9C4}$ (12), $\beta\text{R4}$ (10)
660 <b>654</b>	56	650	61	$\tau\text{R5}$ (45), $\gamma\text{N1H}$ (30), $\tau\text{RR}$ (12), $\tau\text{R4}$ (10)
640	1	636	0	$\tau\text{R4}$ (51), $\gamma\text{N1H}$ (17), $\gamma\text{CO}$ (14), $\tau\text{R3}$ (11)
<b>599</b> 595	13	587	11	$\beta\text{CO}$ (25), $\nu\text{C6N1}$ (23), $\beta\text{R5}$ (18)
545 <b>542</b>	12	536	18	$\tau\text{R2}$ (39), $\tau\text{R1}$ (27), $\tau\text{R5}$ (26), $\gamma\text{N1H}$ (10)
522	1	518	3	$\beta\text{R2}$ (35), $\beta\text{R5}$ (14), $\nu\text{N9C14}$ (11), $\beta\text{N9C14}$ (10)
		504	2	$\beta\text{R3}$ (69), $\beta\text{R2}$ (11)
		352	4	$\beta\text{CO}$ (41), $\beta\text{N9C14}$ (19), $\nu\text{C5C6}$ (16)
		267	0	$\tau\text{R3}$ (62), $\gamma\text{N9C14}$ (22)
		246	1	$\tau\text{RR}$ (55), $\gamma\text{N9C14}$ (24)
		224	1	$\beta\text{N9C14}$ (51), $\beta\text{R2}$ (11)
		170	12	$\tau\text{R2}$ (35), $\tau\text{R3}$ (30), $\gamma\text{N9C14}$ (18), $\tau\text{RR}$ (14)
		109	0	$\gamma\text{N9C14}$ (29), $\tau\text{R2}$ (24), $\tau\text{R1}$ (21)
		50	0	$\tau\text{Me}$ (95)

Wavenumbers of the strongest components of split bands are bold.

<sup>a</sup> Relative integrated intensities.

<sup>b</sup> Theoretical positions of absorption bands were scaled down by a factor of 0.98.

<sup>c</sup> PED's lower than 10% are not included. Definition of internal coordinates is given in Table S2. See Scheme 1 for atom numbering.

Ar matrix (Fig. 5), two bands were observed. The high-intensity band, assigned to the N1H stretching vibration was found at the frequency  $3433\text{ cm}^{-1}$ , similar to the frequencies of analogous bands in the spectra of allopurinol and 4(3H)-pyrimidinone. The lower-intensity band was detected at the frequency  $3557\text{ cm}^{-1}$ , characteristic of the stretching vibration of the OH group. This

picture strongly suggests that two tautomeric forms of 9-methylhypoxanthine were trapped into a low-temperature Ar matrix. Based on the observed ratio of intensities of the experimental  $\nu\text{OH}$  and  $\nu\text{NH}$  bands and taking into account the calculated absolute intensities of these bands, equal 106 and  $68\text{ km mol}^{-1}$ , respectively, the ratio of populations of the oxo

Table 6  
Experimental wavenumbers ( $\tilde{\nu}/\text{cm}^{-1}$ ) and relative integral intensities ( $I$ ) of the absorption bands in the spectrum of the hydroxy form of 9-methylhypoxanthine isolated in an Ar matrix, compared with wavenumbers ( $\tilde{\nu}/\text{cm}^{-1}$ ), absolute intensities ( $A^{\text{th}}/\text{km mol}^{-1}$ ) and potential energy distribution (PED, %) calculated for the oxo form mHxIIa

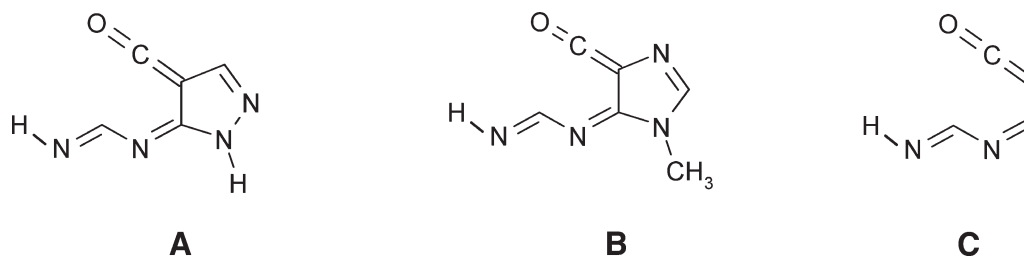
Experimental Ar matrix		Calculated B3LYP/6-31++G(d,p)		
$\tilde{\nu}$	$I^a$	$\tilde{\nu}^b$	$A^{\text{th}}$	PED <sup>c</sup> (%)
3577 3563 <b>3557</b>	100	3682	106	$\nu\text{OH}$ (100)
		3185	0	$\nu\text{C8H}$ (99)
2995	6	3137	14	$\nu\text{C2H}$ (100)
2963	11	3093	7	$\nu\text{Me2}$ (99)
2924	13	3072	9	$\nu\text{Me3}$ (99)
2801	15	3001	38	$\nu\text{Me1}$ (99)
1639 <b>1636</b>	98	1633	224	$\nu\text{C5C6}$ (39)
1585	120	1586	180	$\nu\text{N3C4}$ (26), $\nu\text{C4C5}$ (22), $\nu\text{N1C2}$ (10)
1520	69	1517	57	$\nu\text{N7C8}$ (21), $\beta\text{C8H}$ (17), $\beta\text{R5}$ (11)
1490	6			
1478	26	1489	36	$\beta\text{Me2}$ (74), $\beta\text{Me3}$ (13)
1471 <b>1468</b> 1467	100	1472	132	$\beta\text{C2H}$ (31), $\nu\text{C6N1}$ (23), $\nu\text{CO}$ (12), $\nu\text{C2N3}$ (11)
1447	19	1454	11	$\beta\text{Me4}$ (90)
1430	18	1441	15	$\beta\text{Me1}$ (42), $\nu\text{N7C8}$ (31)
1413	26	1417	26	$\beta\text{Me1}$ (46), $\nu\text{N9C14}$ (15), $\nu\text{N7C8}$ (10)
1361	31	1363	37	$\beta\text{C2H}$ (41), $\nu\text{C6N1}$ (11)
1347	34	1345	55	$\nu\text{C5N7}$ (15), $\nu\text{N7C8}$ (13), $\nu\text{C4C5}$ (12), $\nu\text{C2N3}$ (10), $\nu\text{C8N9}$ (10)
1327 <b>1318</b> 1313	147	1330	169	$\nu\text{C2N3}$ (19), $\nu\text{C8N9}$ (14), $\nu\text{CO}$ (12)
1307	19	1323	10	$\nu\text{N1C2}$ (26), $\nu\text{C2N3}$ (16), $\nu\text{CO}$ (14), $\beta\text{C2H}$ (10)
<b>1282</b> 1272	11	1289	15	$\beta\text{OH}$ (33), $\nu\text{C5N7}$ (23), $\nu\text{N1C2}$ (15)
1236 1235	31	1243	27	$\beta\text{C8H}$ (41), $\nu\text{N7C8}$ (11), $\beta\text{Me3}$ (10)
<b>1213</b> 1207	43	1204	55	$\nu\text{N9C14}$ (17), $\beta\text{C8H}$ (17)
1192	6			
1126	7	1127	1	$\beta\text{Me5}$ (89), $\beta\text{Me4}$ (10)
<b>1111</b> 1109 1107	58	1111	98	$\beta\text{OH}$ (27), $\nu\text{N1C2}$ (20), $\nu\text{C6N1}$ (20)
1052 <b>1050</b>	12	1045	8	$\beta\text{Me3}$ (50), $\nu\text{C8N9}$ (28)
1023 <b>1022</b>	86	1019	99	$\beta\text{R4}$ (25), $\nu\text{CO}$ (16), $\nu\text{N9C14}$ (10), $\beta\text{R5}$ (10)
952	4	946	5	$\gamma\text{C2H}$ (108)
<b>894</b> 889	9	887	8	$\beta\text{R1}$ (43), $\beta\text{R2}$ (15)
855	2	845	7	$\gamma\text{C8H}$ (100)
<b>809</b> 803 802	24	786	12	$\tau\text{R1}$ (52), $\tau\text{R4}$ (22), $\gamma\text{CO}$ (18)
735	6	731	5	$\nu\text{N9C14}$ (21), $\beta\text{R2}$ (17), $\nu\text{C8N9}$ (10), $\beta\text{R4}$ (10)
727	5			
718	12	714	11	$\beta\text{R4}$ (29), $\nu\text{N3C4}$ (13), $\nu\text{C5C6}$ (12)
686	2	677	7	$\gamma\text{CO}$ (49), $\tau\text{R3}$ (14), $\tau\text{R5}$ (11), $\tau\text{RR}$ (11), $\tau\text{R4}$ (10)
647 <b>646</b>	33	644	40	$\tau\text{R4}$ (52), $\tau\text{R5}$ (32)
		592	2	$\beta\text{R5}$ (25), $\beta\text{CO}$ (25)
535	4	560	2	$\tau\text{R2}$ (32), $\tau\text{R5}$ (28), $\tau\text{R1}$ (24)
<b>515</b> 512	45	540	89	$\tau\text{OH}$ (88)
		529	4	$\beta\text{R3}$ (35), $\nu\text{N9C14}$ (12), $\beta\text{R2}$ (11), $\beta\text{N9C14}$ (10)
		520	1	$\beta\text{R3}$ (35), $\beta\text{R2}$ (34)
		331	10	$\beta\text{CO}$ (49), $\beta\text{N9C14}$ (22)
		298	0	$\tau\text{R3}$ (63), $\tau\text{R5}$ (11)
		253	1	$\tau\text{RR}$ (48), $\gamma\text{N9C14}$ (32)
		220	5	$\beta\text{N9C14}$ (49), $\beta\text{R2}$ (10)
		190	1	$\tau\text{R2}$ (47), $\gamma\text{N9C14}$ (24), $\tau\text{RR}$ (17)
		110	5	$\gamma\text{N9C14}$ (34), $\tau\text{R2}$ (23), $\tau\text{R1}$ (10)
		13	0	$\tau\text{Me}$ (96)

Wavenumbers of the strongest components of split bands are bold.

<sup>a</sup> Relative integrated intensities.

<sup>b</sup> Theoretical positions of absorption bands were scaled down by a factor of 0.98.

<sup>c</sup> PED's lower than 10% are not included. Definition of internal coordinates is given in Table S2. See Scheme 1 for atom numbering.



Scheme 3. Open-ring conjugated ketene products photogenerated from (A) allopurinol, (B) 9-methylhypoxanthine and (C) 4(3*H*)-pyrimidinone.

and hydroxy tautomers was estimated as 11.7:1. Eq. (1) was used for this purpose:

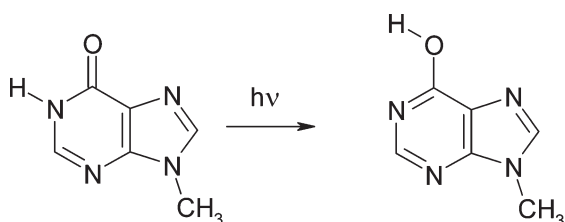
$$\frac{[\text{oxo}]}{[\text{hydroxy}]} = \frac{I(\nu\text{NH})A^{\text{th}}(\nu\text{OH})}{I(\nu\text{OH})A^{\text{th}}(\nu\text{NH})}, \quad (1)$$

where  $I$  is the experimental integrated absorbance, and  $A^{\text{th}}$  is the calculated absolute intensity.

Assuming that the relative population of 9-methylhypoxanthine isomers, characteristic of the gaseous phase equilibrium prior to deposition, is retained in the matrix, it is possible to estimate the difference in energies between the two forms. The temperature of the oven used for deposition of 9-methylhypoxanthine in this study was equal to ca. 480 K. At this temperature the observed ratio of conformers (11.7:1) corresponds, according to the Boltzmann distribution, to the energy difference of 9.8 kJ mol<sup>-1</sup>. This value is in a good correspondence with the energy difference 10.3 kJ mol<sup>-1</sup> calculated by MP2 approach (see Table 4).

UV ( $\lambda > 270$  nm) irradiation of the matrix-isolated monomers of 9-methylhypoxanthine led to the decrease of the bands belonging to the spectrum of the oxo form and to the increase of the (initially very weak) bands of the spectrum of the hydroxy tautomer (Fig. 5). Having two spectra (recorded before and after UV irradiation) of matrices containing different relative populations of the oxo-N(1)H and the hydroxy forms of 9-methylhypoxanthine, it was possible to separate (using numerical subtraction) the spectra of the two tautomers of the compound.

These separated spectra are compared (in Figs. 6 and 7) with the spectra calculated (at the DFT(B3LYP)/6-31++G(d,p) level) for tautomers mHxI and mHxII. Identification of the substrate of the photoreaction as form mHxI and the photoproduct as tautomer mHxII is strongly supported by the good agreement between the experimental and theoretical IR spectra. Hence, the main photochemical process observed for monomeric 9-methylhypoxanthine can be reliably interpreted as a proton transfer mHxI  $\rightarrow$  mHxII reaction (Scheme 4). The assignment of the experimental



Scheme 4. Phototautomeric reaction observed for 9-methylhypoxanthine.

absorption bands in the spectra of both tautomers to the theoretically calculated normal modes is given in Tables 5 and 6.

It does not seem very likely that both rotamers mHxIIa and mHxIIb are generated upon UV irradiation. The theoretically predicted spectrum of form mHxIIb does not reproduce well the experimental spectrum of the photoproduct(s) (see the comparison shown in Fig. 7). Form mHxIIb is predicted to be higher in energy by 5 kJ mol<sup>-1</sup>, with respect to form mHxIIa and the barrier between these two forms was calculated (at the DFT (B3LYP)/6-31++G(d,p) level) to be 35 kJ mol<sup>-1</sup>.

Similarly as it was in the case of allopurinol, photogeneration of a small amount of the open-ring conjugated ketene (Scheme 3B) occurred also for 9-methylhypoxanthine. This form was detected thanks to the high-absolute-intensity band emerging at the characteristic frequency 2151 cm<sup>-1</sup> (Fig. 4).

#### 4.3. Reversibility of the phototautomeric reaction

The phototautomeric reactions observed for allopurinol and 9-methylhypoxanthine did not lead to the total conversion of the

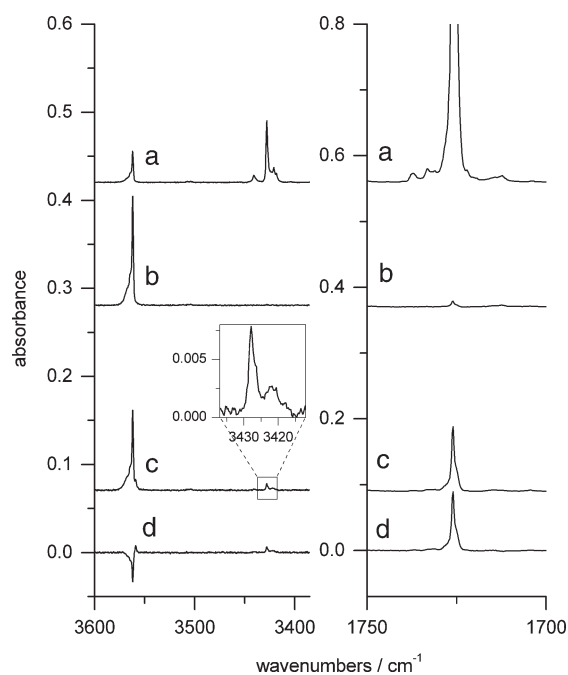
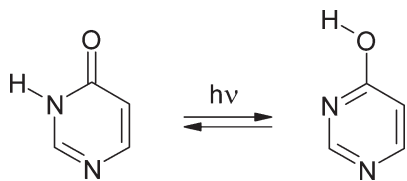


Fig. 8. Portions of the IR spectra of 4(3*H*)-pyrimidinone isolated in an Ar matrix: (a) after deposition of the matrix; (b) after UV irradiation with  $\lambda > 270$  nm; (c) after UV irradiation with  $\lambda > 230$  nm; (d) difference spectrum: trace c minus trace b.



Scheme 5. Phototautomeric reaction observed for 4(3H)-pyrimidinone.

initial oxo forms of the compounds into the corresponding hydroxy forms. One of the possible reasons for that can be the reversibility of the oxo  $\leftrightarrow$  hydroxy phototransformations. This could happen if (together with the photoreaction transforming the oxo forms of the compounds into the hydroxy tautomer) a concomitant hydroxy  $\rightarrow$  oxo phototransformation occurred. In such a case the observed photoprocess would lead to a photo-stationary state.

Photoreversibility of the oxo–hydroxy phototautomerism of the type observed for allopurinol and 9-methylhypoxanthine was experimentally proven in the current work for the model system 4(3H)-pyrimidinone/4-hydroxypyrimidine. This model molecule has only a six-membered ring and the possibility of the tautomerism involving pyrazole or imidazole ring is automatically excluded.

Both oxo and hydroxy forms of this model compound are populated in the gas phase and are trapped into a low-temperature Ar matrix [38,39]. Irradiation of matrix-isolated 4(3H)-pyrimidinone with UV ( $\lambda > 270$  nm) light led to an almost total conversion of the oxo form into the hydroxy tautomer (Fig. 8). Upon subsequent UV ( $\lambda > 230$  nm) irradiation partial recovery of the oxo tautomer occurred (Fig. 8, traces b, c, d). The spectral signature of this reverse hydroxy  $\rightarrow$  oxo photoprocess is the reappearance and increase of the  $\nu$ NH band (at  $3428\text{ cm}^{-1}$ ) and the  $\nu$ C=O band (at  $1726\text{ cm}^{-1}$ ), both characteristic of the IR spectrum of the oxo tautomer [40]. This direct observation provides the first case of the oxo–hydroxy phototautomerism (of the type discussed in the present paper, see Scheme 5), for which the photoreversibility is unequivocally proven.

## 5. Conclusions

The infrared spectra of monomers of allopurinol and 9-methylhypoxanthine isolated in low-temperature Ar matrices are reported for the first time. These spectra were interpreted by comparison with the IR spectra theoretically calculated for all possible tautomeric forms of these molecules at the DFT(B3LYP)/6-311++G(d,p) level. This comparison revealed that allopurinol adopts the oxo-N(1)H,N(5)H form (AI). The oxo-N(1)H form (mHxI) is dominant in the case of 9-methylhypoxanthine, however a small amount (ca. 8%) of the hydroxy tautomer (mHxII) was also detected.

UV illumination of both compounds resulted in transformation of the initially abundant oxo forms into the corresponding hydroxy tautomers (Schemes 2 and 4). The photogenerated species were identified on the basis of a good agreement between their IR spectra and the spectra calculated for the AIIIa and mHxIIa hydroxy tautomers.

The vibrational spectra of the reagents (oxo tautomers) and the photoproducts (hydroxy tautomers) were assigned to the theoretically calculated normal modes.

The phototautomeric reaction of the same type occurred also for the model compound 4(3H)-pyrimidinone/4-hydroxypyrimidine (Scheme 5). For this species, illumination with UV ( $\lambda > 270$  nm) converted the oxo form to the hydroxy tautomer. Subsequent irradiation with the light of shorter wavelengths ( $\lambda > 230$  nm) led to partial repopulation of the oxo tautomer. This was the first experimental observation of the photoreversibility of the oxo–hydroxy intramolecular phototautomerization in the compounds where the hydrogen atom is shifted between the N–H and C=O groups placed at alpha position with respect to each other.

## Acknowledgments

The authors express their gratitude to Professor Bernhard Lippert (Universität Dortmund, Germany) for providing them with a sample of 9-methylhypoxanthine. I. R. and A.G. acknowledge the support of the Centre of Excellence ASPECT financed by the European Commission within the contract G6MA-CT-2002-04021.

## Appendix A. Supplementary data

Supplementary data associated with this article can be found, in the online version, at [doi:10.1016/j.bpc.2006.03.002](https://doi.org/10.1016/j.bpc.2006.03.002).

## References

- [1] L. Stryer, Biochemistry, fourth edition, W.H. Freeman and Company, New York, 1995.
- [2] S.K. Mitra, J. Ninio, Recognition between codon and anticodon, The limits of our knowledge, FEBS Symp. 51 (1978) 437–444.
- [3] J.L. Smith, Enzymes of nucleotide synthesis, Curr. Opin. Struct. Biol. 5 (1995) 752–757.
- [4] A. Wakai, Desmond C. Winter, John T. Street, Ronan G. O'Sullivan, Jiang H. Wang, H. Paul Redmond, Inosine attenuates tourniquet-induced skeletal muscle reperfusion injury, J. Surg. Res. 99 (2001) 311–315.
- [5] R.L. Wortmann, Recent advances in the management of gout and hyperuricemia, Curr. Opin. Rheumatol. 17 (2005) 319–324.
- [6] R.L. Wortmann, Gout and hyperuricemia, Curr. Opin. Rheumatol. 14 (2002) 281–286.
- [7] E. Pea, Pharmacology of drugs for hyperuricemia — mechanisms, kinetics and interactions, Contrib. Nephrol. 147 (2005) 35–46.
- [8] G. Bellinghieri, D. Santoro, V. Savica, Pharmacological treatment of acute and chronic hyperuricemia in kidney diseased patients, Contrib. Nephrol. 147 (2005) 149–160.
- [9] B.T. Emmerson, Drug therapy — the management of gout, New Engl. J. Med. 334 (1996) 445–451.
- [10] N. Schlesinger, Management of acute and chronic gouty arthritis — present state-of-the-art, Drugs 64 (2004) 2399–2416.
- [11] M.S. Cairo, M. Bishop, Tumour lysis syndrome: new therapeutic strategies and classification, Br. J. Haematol. 127 (2004) 3–11.
- [12] M.T. Holdsworth, P. Nguyen, Role of i.v. allopurinol and rasburicase in tumor lysis syndrome, Am. J. Health-Syst. Pharm. 60 (2003) 2213–2222.
- [13] H. Adachi, K. Motomatsu, I. Yara, Effect of allopurinol (zyloric) on patients undergoing open heart surgery, Jpn. Circ. J. 43 (1979) 395–401.
- [14] F. Mellin, C. Monteil, M. Isabelle, B. Di Melgio, J.P. Henry, C. Thuillez, P. Mulder, Long-term allopurinol treatment initiated in well established

- chronic heart failure improves cardiac function and structure, *Free Radic. Biol. Med.* 37 (Suppl. 1) (2004) S39.
- [15] W. Guan, T. Osanai, T. Kamada, H. Hanada, H. Ishizaka, H. Onodera, A. Iwasa, N. Fujita, S. Kudo, T. Ohkubo, K. Okumura, Effect of allopurinol pretreatment on free radical generation after primary coronary angioplasty for acute myocardial infarction, *J. Cardiovasc. Pharmacol.* 41 (2003) 699–705.
- [16] N.A. Weimert, W.F. Tanke, J.J. Sims, Allopurinol as a cardioprotectant during coronary artery bypass graft surgery, *Ann. Pharmacother.* 37 (2003) 1708–1711.
- [17] A. Movahed, K. Nair, T.F. Ashavaid, P. Kumar, Free radical generation and role of allopurinol as a cardioprotective agent during coronary artery bypass grafting surgery, *Can. J. Cardiol.* 12 (1996) 138–144.
- [18] R. Machado-Vieira, F. Kapczinski, D.O. Souza, D.R. Lara, J.C. Soares, A double-blind controlled study of adjunctive allopurinol or dipyridamole to lithium in the treatment of bipolar mania: preliminary results, *Bipolar Disord.* 7 (Suppl. 2) (2005) 73.
- [19] S. Akhondzadeh, A. Safarcherati, H. Amini, Beneficial antipsychotic effects of allopurinol as add-on therapy for schizophrenia: a double blind, randomized and placebo controlled trial, *Prog. Neuro-Psychopharmacol.* 29 (2005) 253–259.
- [20] P. Prusiner, M. Sundaralingam, Stereochemistry of nucleic acids and their constituents, XXIX, Crystal and molecular structure of allopurinol, a potent inhibitor of xanthine oxidase, *Acta Crystallogr., B* 28 (1972) 2148–2152.
- [21] M.K. Shukla, P.C. Mishra, Electronic spectra and structure of allopurinol: a xanthine oxidase inhibitor, *Spectrochim. Acta, Part A* 52 (1996) 1547–1557.
- [22] A. Torreggiani, M. Tamba, A. Trincherio, G. Fini, A spectroscopic and pulse radiolysis study of allopurinol and its copper complex, *J. Mol. Struct.* 651–653 (2003) 91–99.
- [23] M.T. Chenon, R.J. Pugmire, D.M. Grant, R.P. Panzica, L.B. Townsend, Carbon-13 NMR spectra of C-Nucleosides, II, A study on the tautomerism of formycin and formycin B by the use of CMR spectroscopy, *J. Heterocycl. Chem.* 10 (1973) 431–433.
- [24] R.H. Fish, G. Jaouen, Bioorganometallic chemistry: structural diversity of organometallic complexes with bioligands and molecular recognition studies of several supramolecular hosts with biomolecules, alkali–metal ions, and organometallic pharmaceuticals, *Organometallics* 22 (2003) 2166–2177.
- [25] E. Freisinger, I.B. Rother, M.S. Lüth, B. Lippert, Canonical and unconventional pairing schemes between bis(nucleobase) complexes of *trans*-a2P<sub>III</sub>: artificial nucleobase quartets and COH $\cdots$ N bonds, *PNAS* 100 (2003) 3748–3753.
- [26] J. Lin, C. Yu, S. Peng, I. Akiyama, K. Li, Li Kao Lee, P.R. LeBreton, Ultraviolet photoelectron studies of the ground-state electronic structure and gas-phase tautomerism of hypoxanthine and guanine, *J. Phys. Chem.* 84 (1980) 1006–1012.
- [27] A.R.I. Munns, P. Tollin, The crystal and molecular structure of inosine, *Acta Crystallogr., B* 26 (1970) 1101–1113.
- [28] A. Becke, Density-functional exchange-energy approximation with correct asymptotic behavior, *Phys. Rev., A* 38 (1988) 3098–3100.
- [29] C.T. Lee, W.T. Yang, R.G. Parr, Development of the Colle–Salvetti correlation-energy formula into a functional of the electron density, *Phys. Rev., B* 37 (1988) 785–789.
- [30] J.H. Schachtschneider, Technical Report, Shell Development Co., Emeryville, CA, 1969.
- [31] P. Pulay, G. Fogarasi, F. Pang, J.E. Boggs, Systematic ab initio gradient calculation of molecular geometries, force constants, and dipole moment derivatives, *J. Am. Chem. Soc.* 101 (1979) 2550–2560.
- [32] G. Keresztury, G. Jalsovszky, An alternative calculation of the vibrational potential energy distribution, *J. Mol. Struct.* 10 (1971) 304–305.
- [33] C. Møller, M.S. Plesset, Note on an approximation treatment for many-electron systems, *Phys. Rev.* 46 (1934) 618–622.
- [34] M.J. Frisch, G.W. Trucks, H.B. Schlegel, G.E. Scuseria, M.A. Robb, J.R. Cheeseman, V.G. Zakrzewski, J.A. Montgomery Jr., R.E. Stratmann, J.C. Burant, S. Dapprich, J.M. Millam, A.D. Daniels, K.N. Kudin, M.C. Strain, O. Farkas, J. Tomasi, V. Barone, M. Cossi, R. Cammi, B. Mennucci, C. Pomelli, C. Adamo, S. Clifford, J. Ochterski, G.A. Petersson, P.Y. Ayala, Q. Cui, K. Morokuma, D.K. Malick, A.D. Rabuck, K. Raghavachari, J.B. Foresman, J. Cioslowski, J.V. Ortiz, A.G. Baboul, B.B. Stefanov, G. Liu, A. Liashenko, P. Piskorz, I. Komaromi, R. Gomperts, R.L. Martin, D.J. Fox, T. Keith, M.A. Al-Laham, C.Y. Peng, A. Nanayakkara, M. Challacombe, P.M.W. Gill, B. Johnson, W. Chen, M.W. Wong, J.L. Andres, C. Gonzalez, M. Head-Gordon, E.S. Replogle, J.A. Pople, Gaussian 98, Revision A.7, Gaussian, Inc., Pittsburgh, PA, 1998.
- [35] B. Hernandez, F.J. Luque, M. Orozco, Tautomerism of xanthine oxidase substrates hypoxanthine and allopurinol, *J. Org. Chem.* 61 (1996) 5964–5971.
- [36] M.E. Costas, R. Acevedo-Chavez, Density functional study of neutral allopurinol tautomeric forms, *J. Comput. Chem.* 20 (1999) 200–206.
- [37] L. Lapinski, M.J. Nowak, A. Les, L. Adamowicz, Comparison of ab initio HF/6-31G\*\*, HF/6-31++G\*\* and MP2/6-31G\*\* calculated infrared spectra of 4(3H)-pyrimidinone and 4-hydroxypyrimidine with matrix isolation spectra, *Vibr. Spectrosc.* 8 (1995) 331–342.
- [38] M.J. Nowak, L. Lapinski, J. Fulara, IR spectra and phototautomerism of matrix isolated 4-oxypyrimidine, *J. Mol. Struct.* 175 (1988) 91–96.
- [39] L. Lapinski, J. Fulara, M.J. Nowak, Infrared matrix isolation and ab initio studies of 4-oxypyrimidine; separation of the spectra of tautomers based on the phototautomeric effect, *Spectrochim. Acta A* 46 (1990) 61–71.
- [40] L. Lapinski, M.J. Nowak, A. Les, L. Adamowicz, Ab initio calculations of IR spectra in identification of products of matrix isolation photochemistry: dewar form of 4(3H)-pyrimidinone, *J. Am. Chem. Soc.* 116 (1994) 1461–1467.
- [41] S. Breda, I. Reva, L. Lapinski, R. Fausto, Matrix isolation FTIR and theoretical study of alpha-pyrone photochemistry, *Phys. Chem. Chem. Phys.* 6 (2004) 929–937.
- [42] R. Ramaekers, G. Maes, L. Adamowicz, A. Dkhissi, Matrix-isolation FT-IR study and theoretical calculations of the vibrational, tautomeric and H-bonding properties of hypoxanthine, *J. Mol. Struct.* 560 (2001) 205–221.
- [43] R. Ramaekers, A. Dkhissi, L. Adamowicz, G. Maes, Matrix-isolation FT-IR study and theoretical calculations of the hydrogen-bond interaction of hypoxanthine with H<sub>2</sub>O, *J. Phys. Chem., A* 106 (2002) 4502–4512.
- [44] M.E. Costas, R. Acevedo-Chavez, Density functional study of the neutral hypoxanthine tautomeric forms, *J. Phys. Chem., A* 101 (1997) 8309–8318.
- [45] M.K. Shukla, J. Leszczynski, A DFT investigation on the effects of hydration on the tautomeric equilibria of hypoxanthine, *J. Mol. Struct., Theochem* 529 (2000) 99–112.